

QC
807.5
.U66
no.319



NOAA TR ERL 319-APCL 33

NOAA Technical Report ERL 319-APCL 33

U.S. DEPARTMENT OF COMMERCE
NATIONAL OCEANIC AND ATMOSPHERIC ADMINISTRATION
Environmental Research Laboratories

Zonal Profiles of Atmospheric Water Vapor

P. M. KUHN

BOULDER, COLO.
MARCH 1975



ENVIRONMENTAL RESEARCH LABORATORIES

The mission of the Environmental Research Laboratories is to study the oceans, inland waters, the lower and upper atmosphere, the space environment, and the earth, in search of the understanding needed to provide more useful services in improving man's prospects for survival as influenced by the physical environment. Laboratories contributing to these studies are:

Atlantic Oceanographic and Meteorological Laboratories (AOML): Geology and geophysics of ocean basins and borders, oceanic processes, sea-air interactions and remote sensing of ocean processes and characteristics (Miami, Florida).

Pacific Marine Environmental Laboratory (PMEL): Environmental processes with emphasis on monitoring and predicting the effects of man's activities on estuarine, coastal, and near-shore marine processes (Seattle, Washington).

Great Lakes Environmental Research Laboratory (GLERL): Physical, chemical, and biological limnology, lake-air interactions, lake hydrology, lake level forecasting, and lake ice studies (Ann Arbor, Michigan).

Atmospheric Physics and Chemistry Laboratory (APCL): Processes of cloud and precipitation physics; chemical composition and nucleating substances in the lower atmosphere; and laboratory and field experiments toward developing feasible methods of weather modification.

Air Resources Laboratories (ARL): Diffusion, transport, and dissipation of atmospheric contaminants; development of methods for prediction and control of atmospheric pollution; geophysical monitoring for climatic change (Silver Spring, Maryland).

Geophysical Fluid Dynamics Laboratory (GFDL): Dynamics and physics of geophysical fluid systems; development of a theoretical basis, through mathematical modeling and computer simulation, for the behavior and properties of the atmosphere and the oceans (Princeton, New Jersey).

National Severe Storms Laboratory (NSSL): Tornadoes, squall lines, thunderstorms, and other severe local convective phenomena directed toward improved methods of prediction and detection (Norman, Oklahoma).

Space Environment Laboratory (SEL): Solar-terrestrial physics, service and technique development in the areas of environmental monitoring and forecasting.

Aeronomy Laboratory (AL): Theoretical, laboratory, rocket, and satellite studies of the physical and chemical processes controlling the ionosphere and exosphere of the earth and other planets, and of the dynamics of their interactions with high-altitude meteorology.

Wave Propagation Laboratory (WPL): Development of new methods for remote sensing of the geophysical environment with special emphasis on optical, microwave and acoustic sensing systems.

Marine EcoSystem Analysis Program Office (MPO): Plans and directs interdisciplinary analyses of the physical, chemical, geological, and biological characteristics of selected coastal regions to assess the potential effects of ocean dumping, municipal and industrial waste discharges, oil pollution, or other activity which may have environmental impact.

Weather Modification Program Office (WMPO): Plans and directs ERL weather modification research activities in precipitation enhancement and severe storms mitigation and operates ERL's research aircraft.

NATIONAL OCEANIC AND ATMOSPHERIC ADMINISTRATION

BOULDER, COLORADO 80302

QC
807.5
-U66
no. 319



U.S. DEPARTMENT OF COMMERCE
Frederick B. Dent, Secretary

NATIONAL OCEANIC AND ATMOSPHERIC ADMINISTRATION
Robert M. White, Administrator
ENVIRONMENTAL RESEARCH LABORATORIES
Wilmot N. Hess, Director

NOAA TECHNICAL REPORT ERL 319-APCL 33

Zonal Profiles of Atmospheric Water Vapor

NOAA CENTRAL LIBRARY

MAR 13 2017

National Oceanic &
Atmospheric Administration
US Dept of Commerce

P. M. KUHN

BOULDER, COLO.
March 1975

For sale by the Superintendent of Documents, U. S. Government Printing Office, Washington, D. C. 20402

73 1037

CONTENTS

	Page
ABSTRACT	1
1.0 INTRODUCTION	1
2.0 INSTRUMENTATION	1
3.0 APPLIED THEORY	3
3.1 Water Vapor Burden	3
3.2 Water Vapor Concentration	5
4.0 OBSERVATIONS	6
5.0 CONCLUSIONS	10
6.0 ACKNOWLEDGEMENTS	10
7.0 REFERENCES	11

ZONAL PROFILES OF ATMOSPHERIC WATER VAPOR

P. M. Kuhn

Water vapor burden and in situ mixing ratios at high altitude flight levels were inferred from observations in the rotational water vapor spectral band (19.0-35.0 μm). Flight levels averaged approximately 14.0 km during twenty-two zonal traverses aboard the NASA Ames Research Center's Airborne Infrared Observatory. The method of radiance observations to infer water vapor burden and concentration, while radiometric, involved emission observations rather than absorption spectra analysis employed by McKinnon and Morewood [1970]. The east-west flights were made during the February through December, 1974, period. They provided profiles of lower stratospheric and upper tropospheric water vapor from 30° to 50° North latitude between 90° and 140° West longitude.

The objective of the research is to describe the method of recovery of the water vapor burden and in situ mixing ratio by inference from infrared emission observations and to present typical results.

1.0 INTRODUCTION

Previous aircraft and balloon borne observations of lower stratospheric water vapor give an average concentration of 2.5 parts per million. Most of the measurements have been obtained from single locations. Mastenbrook [1971, 1974] has, perhaps, acquired the largest number of balloon observations. Brewer and Tomson [1972] have inferred water vapor infrared emission by observations made from a balloon platform. Recently Harries, et al. [1974] observed water vapor burden and in situ concentrations from high altitude aircraft over moderately restricted traverses. However, it was McKinnon and Morewood [op. cit.] who accomplished the first stratospheric water vapor burden observations along an extended traverse from infrared observations. Kuhn, et al. [1971] followed with long traverses around large thunderstorm systems. This work describes a similar set of observations but with a different infrared inference technique.

2.0 INSTRUMENTATION

The radiometer employed in these observations (Figure 1) is a chopper system with a speed of response of 20 ms. The electronic signal is AC from a temperature controlled, deuterated triglycine sulfate pyroelectric detector, referenced to the black chopper. The temperature of the chopper blade is monitored by a thermistor bead embedded in the chopper. Connections to the thermistor are made through redundant slip rings.

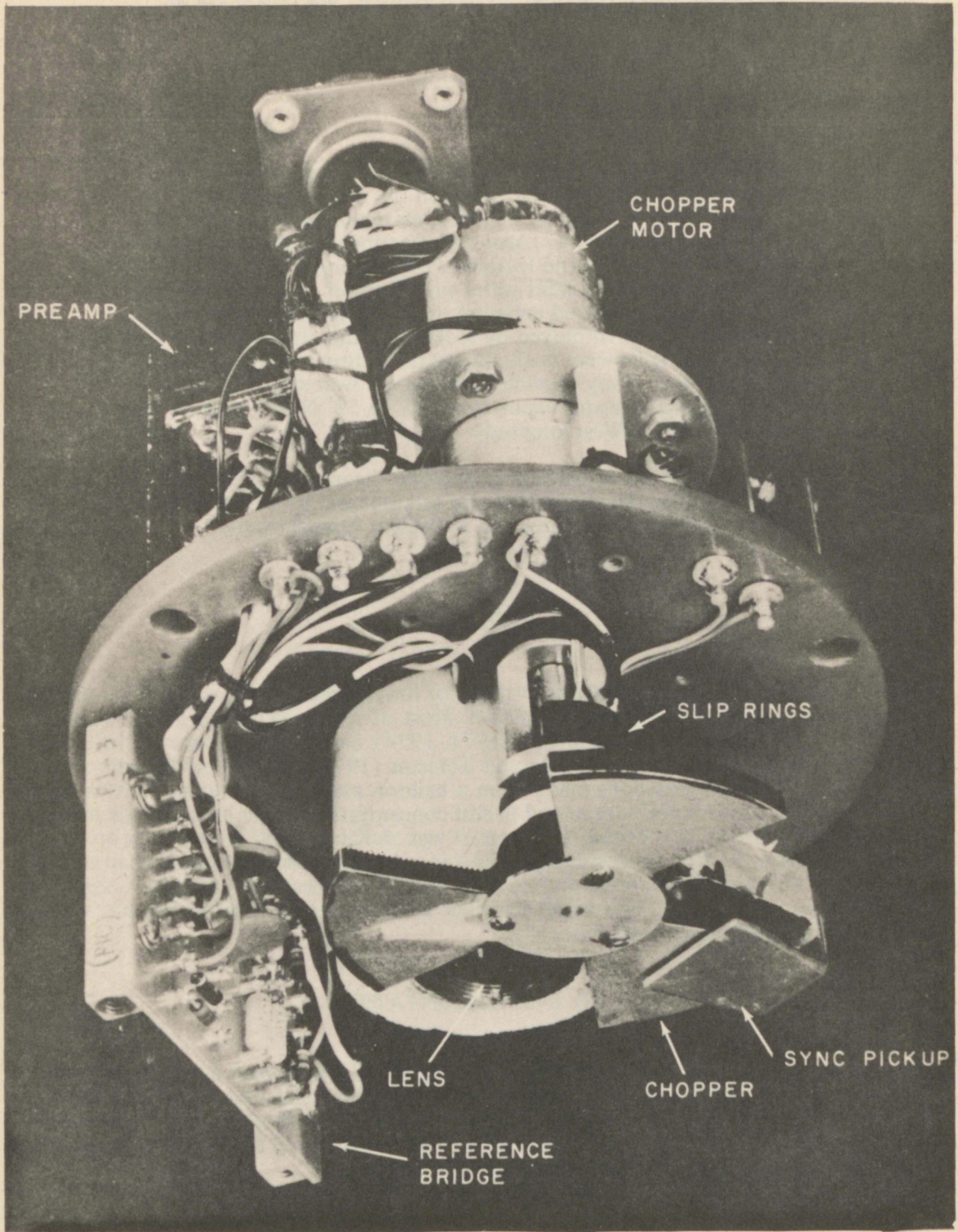


Figure 1. Water vapor radiometric optical head.

The radiometer forward lens is silicon. The aft interference filter is an optical flat of coated silicon with a cut-on frequency of 512 cm^{-1} and a peak transmission of 0.58 decreasing to 0.05 at 266 cm^{-1} . The noise equivalent radiance (N.E. Δ N.) of the radiometer system was measured to be $2.1 \times 10^{-7} \text{ w cm}^{-2} \text{ sr}^{-1}$ at the detector. Electronic output is -10.0 to +10.0 VDC.

To ascertain the minimum detectable water vapor burden at a flight level of 19.0 km (60 mb) a reference to Table 1 calculations is necessary. This data represents a calculation of downward radiance for the spectral interval of the radiometer employed. Recalling the instrument N.E. Δ N. of 2.1×10^{-7} and comparing the water vapor burden and radiance at 50.0 and 70.0 mb reveals a radiance differential of $5.5 \times 10^{-7} \text{ w cm}^{-2} \text{ sr}^{-1}$ corresponding to a water vapor burden differential of approximately $\pm 0.2 \times 10^{-4} \text{ w cm}^{-2} \text{ sr}^{-1}$. If we arbitrarily double this "error" response, arriving at $\pm 0.4 \times 10^{-4} \text{ w cm}^{-2} \text{ sr}^{-1}$ it is evident that our percentage error for observations at 60 mb is 20 percent (0.4/2.0).

3.0 APPLIED THEORY

3.1 Water Vapor Burden

The following five equations with appropriate directions are the technique by which we proceed from observed radiance, to calculated radiance, to inferred water vapor burden. Before following the plan of the inference we should state three basic assumptions:

1. A temperature profile above the aircraft is assumed using the nearest sounding station, but based on an observed flight level temperature.
2. The latest water vapor transmission functions [Wark, et al. 1974] are employed as valid for the atmosphere.
3. The water vapor mixing ratio lapse with height above observational level follows a power law [Smith, 1966].

Basically an iterative routine is employed to minimize the difference between the observed downward radiance $N_o \downarrow$ and the calculated radiance $N_c \downarrow$. It follows that

$$(N_c \downarrow - N_o \downarrow) \Delta \nu \leq \text{N.E.}\Delta\text{N.} (2.1 \times 10^{-7} \text{ w cm}^{-2} \text{ sr}^{-1}), \quad (1)$$

where $\Delta \nu$ is the radiometer response frequency interval, 266-512 cm^{-1} .

Calculated or observed downward radiance may be expressed as:

$$N \downarrow = \iint_{\nu p} \phi(\nu) B(\nu, T(p) \dots) \frac{\partial \tau(u, (p), \nu)}{\partial p} dp d\nu \quad (\text{w cm}^{-2} \text{ sr}^{-1}) \quad (2)$$

where p is pressure (mb),
 ϕ is radiometer system transmission,
 B is the Planck function,
 τ is the transmission function of water vapor (266-512 cm^{-1}),
 u is the optical mass of water vapor (g cm^{-2}),
 T is the absolute temperature ($^{\circ}\text{K}$), and
 ν is the frequency (cm^{-1}).

Defining the temperature profile above flight level it is possible to vary the downward radiance, N_{\downarrow} , by varying $u(p)$, since,

$$\tau = \tau(u, k). \quad (3)$$

Here k is the water vapor absorption coefficient, ($g \text{ cm}^{-2}$).

The optical mass, u , is varied by changes in the flight level mixing ratio, q_0 , in the mathematical approximation for u , ($g \text{ cm}^{-2}$)

$$u = \frac{1}{g} \int_p \bar{q} dp \approx \frac{1}{gp_0^\lambda} \sum_i q_0 p_i^\lambda \Delta p, \quad (g \text{ cm}^{-2}) \quad (4)$$

where g is the acceleration of gravity (cm sec^{-2})
 q is the water vapor mass mixing ratio ($g \text{ g}^{-1}$)
 $"_0"$ subscript refers to flight or reference level, and
 λ is a power law exponent, 1.8 [Smith, op. cit.]

The choice of a non-zero value for λ eliminates the assumption of a uniform mixing ratio with height. Thus (4) reduces to,

$$u = q_0 C \quad (5)$$

where λ , Δp and p_0 are fixed. In effect Δp is fixed as one assigns 10 mb intervals to Δp upward to 0.1 mb from the pressure, p , at flight level. It is therefore, necessary to change only q_0 as part of an iterative convergence routine for $N_{c\downarrow}$ and $N_{o\downarrow}$. The technique used is a modified Newton-Raphson solution (to alter u from the i -th to $i+1$ -th iteration). It is due to Ralston and Wilf [1967].

In essence, then, one defines a temperature profile above radiometer flight level, makes an educated first guess of q_0 at flight level, p , and proceeds to minimize the difference between $N_{c\downarrow}$ and $N_{o\downarrow}$ via the iterative calculation to which we alluded.

3.2 Water Vapor Concentration

The water vapor concentration is an automatic output from the solution of (5). It appears as a solution of this equation along with the total water vapor and as stated does not imply a constant mixing ratio above the aircraft.

4.0 OBSERVATIONS

Of the numerous flights made during 1974 and 1975, two in particular typify the results of what was a successful series of observations. It was in the latter missions, October through December, that it was possible to infer the water vapor concentration at or very near flight level in addition to the burden of water vapor above the aircraft.

On the 31st of December 1974 centered on approximately 1000 UT a long infrared astronomical mission of the C-141-A provided at least three-and-one-half hours of flight time above the tropopause at 13.44 km. During this mission there were two crossings of the sub-polar jet and a penetration into both the subsiding east side of the eastern Pacific sub-tropical high-pressure center and an on-shore trough system.

From a position near Cheyenne, the commencing of the westward leg, the track, initiated at 0528 UT, is superimposed on the 1000 UT 200 mb contour chart (Fig. 2). Here the 200 mb height contours, the temperature field and the general flow pattern indicating the eastern Pacific high and a deep trough along the West Coast are displayed. Strong subsidence is evident from the water vapor burdens along the flight track. In fact the burden drops to $1.4 \times 10^{-4} \text{ g cm}^{-2}$ near the core of the jet.

The southwest track, deeper into the ridge, reflects a decrease in subsidence and a stronger upward flux of moisture from the marine layer, reaching $7.7 \times 10^{-4} \text{ g cm}^{-2}$.

The eastward leg, terminating with the descent at 0932 UT, displays the strong, winter spatial variation in the water vapor burden as the traverse leaves the Pacific high, crosses the subpolar jet and moves slightly into the trough. Figure 3 is a profile of water vapor burden (1-symbols), aircraft ground speed (2-symbols) and altitude (3-symbols). The dramatic drop in water vapor between 0913 and 0921 and corresponding, but lagging, decrease in the C-141 ground speed indicates strong subsidence and associated turbulence as the atmospheric jet is approached and crossed. This is also a clear indicator that the water vapor spectral band can possibly be used as a CAT forecast. The sharp increase in water vapor from 0921 to 0932 followed by an increase in C-141 ground speed represents the effects of strong mixing into the trough side of the jet.

One should here note that an increase in ground speed at constant level indicates that the aircraft is responding to an updraft while the converse is true for a downdraft. It is a fair measure of turbulence in the absence of accelerometers. This equipment has now been installed on the C-141.

The second flight to be discussed occurred on 5 March 1975 at 0145 UT. The flight level was 41,000 feet (180 mb) on track from Moffett Field to Victorville, Calif., Needles, Calif. and northward along the 114th meridian into southern Montana, Spokane, Wash.-area, eastern Idaho and return to Moffett Field. At this time the subpolar jet was well to the south of the United States. A rather deep low was centered at 33°N latitude by 132°W longitude. The eastern Pacific high cell was well to the west of the low. By virtue of the position of the West Coast low and the flight track from south to north two distinctly different air masses were traversed on the mission. Figure 4 superimposes the aircraft path on the 00 UT, 05 March 1975 200 mb contour, isotach and temperature chart. Over the Spokane and northern Idaho portion of the operation the upper air flow was from the northwest originating over the Gulf of Alaska. It also displayed some ridging. In agreement, water vapor burden values were typical of an air mass originating in northern latitudes and displaying low subsidence. Average values were approximately $4.1 \times 10^{-4} \text{ g cm}^{-2}$.

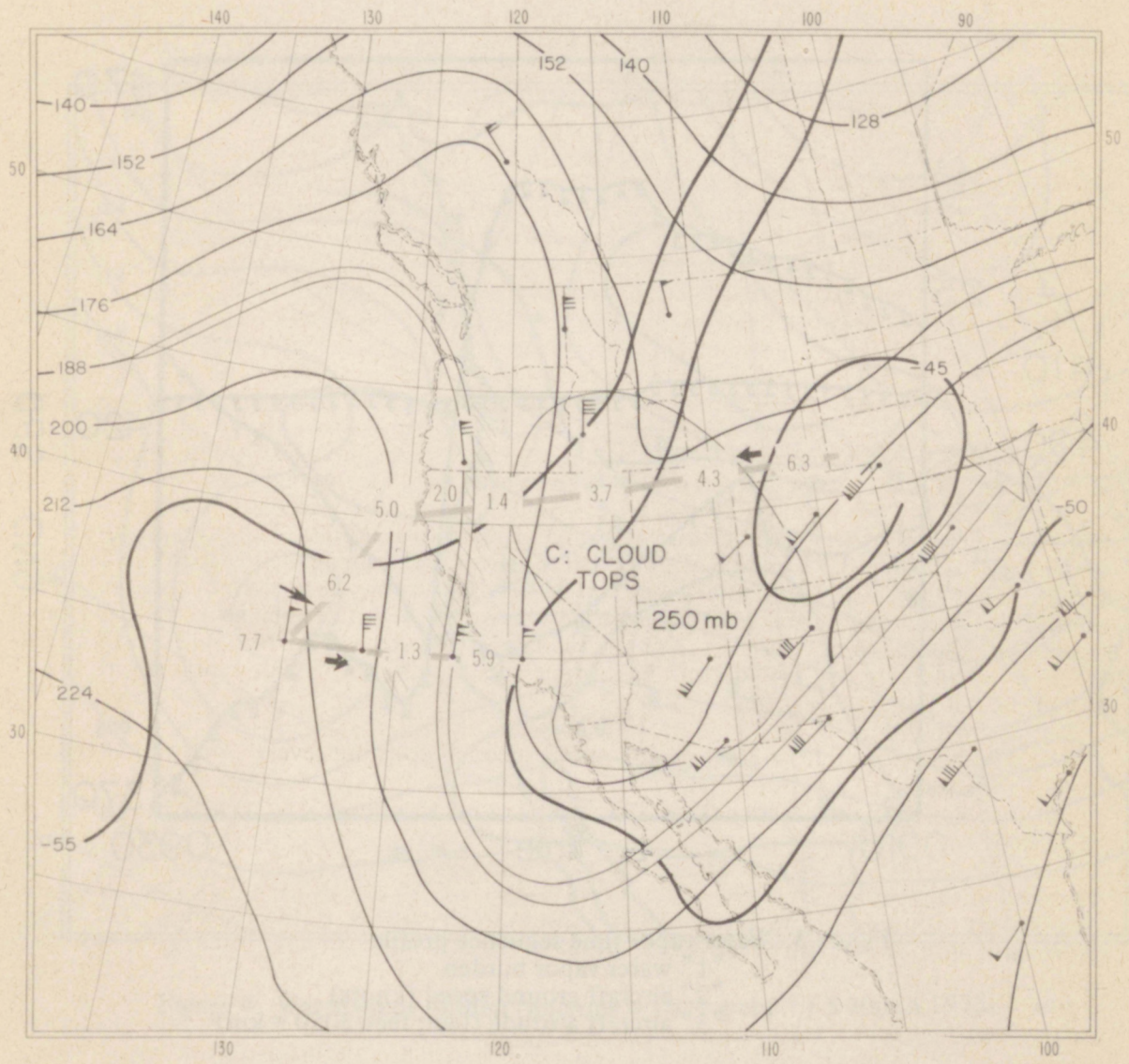


Figure 2. Water vapor burden (microns $\equiv 10^{-4} \text{ g cm}^{-2}$)
 31 December 1974

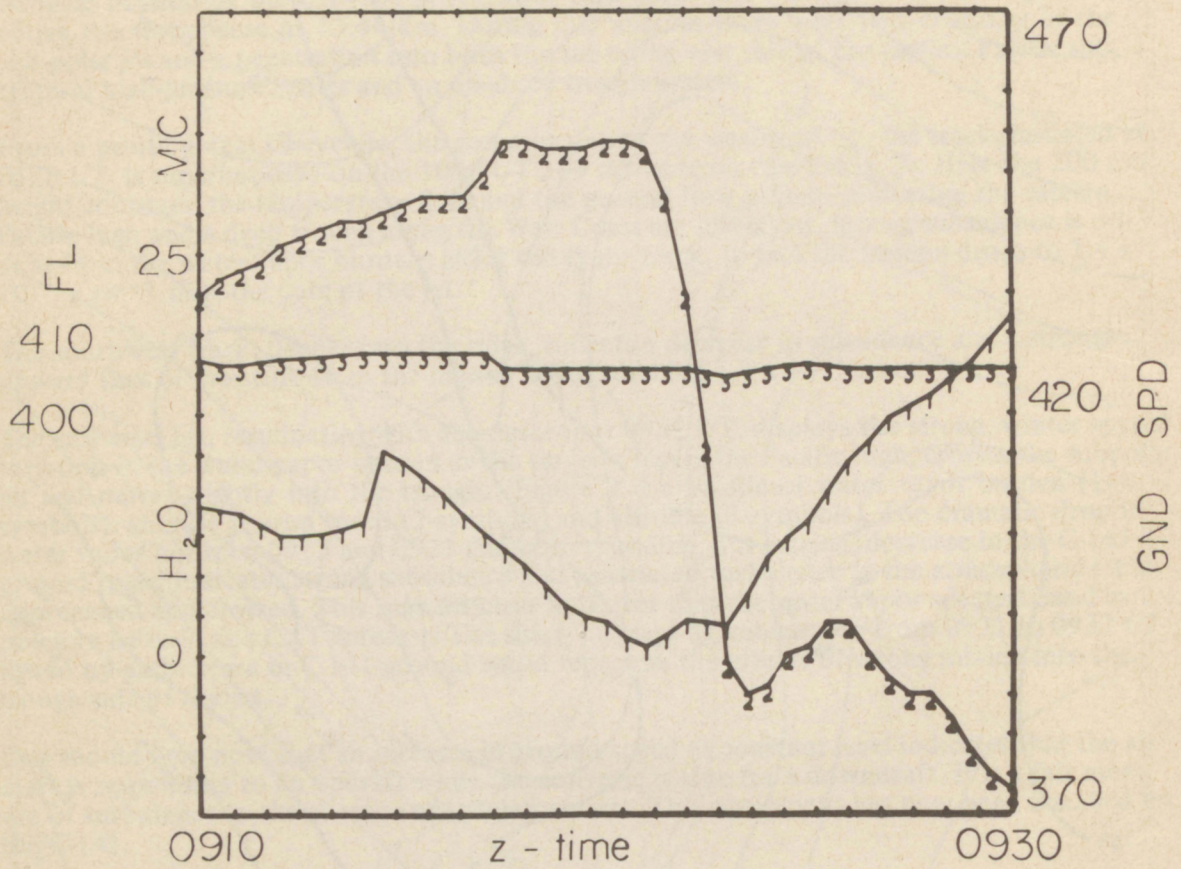


Figure 3. Water vapor time sequence profile
 "1" water vapor burden
 "2" aircraft ground speed (knots)
 "3" aircraft altitude (feet; feet/3050 = km)

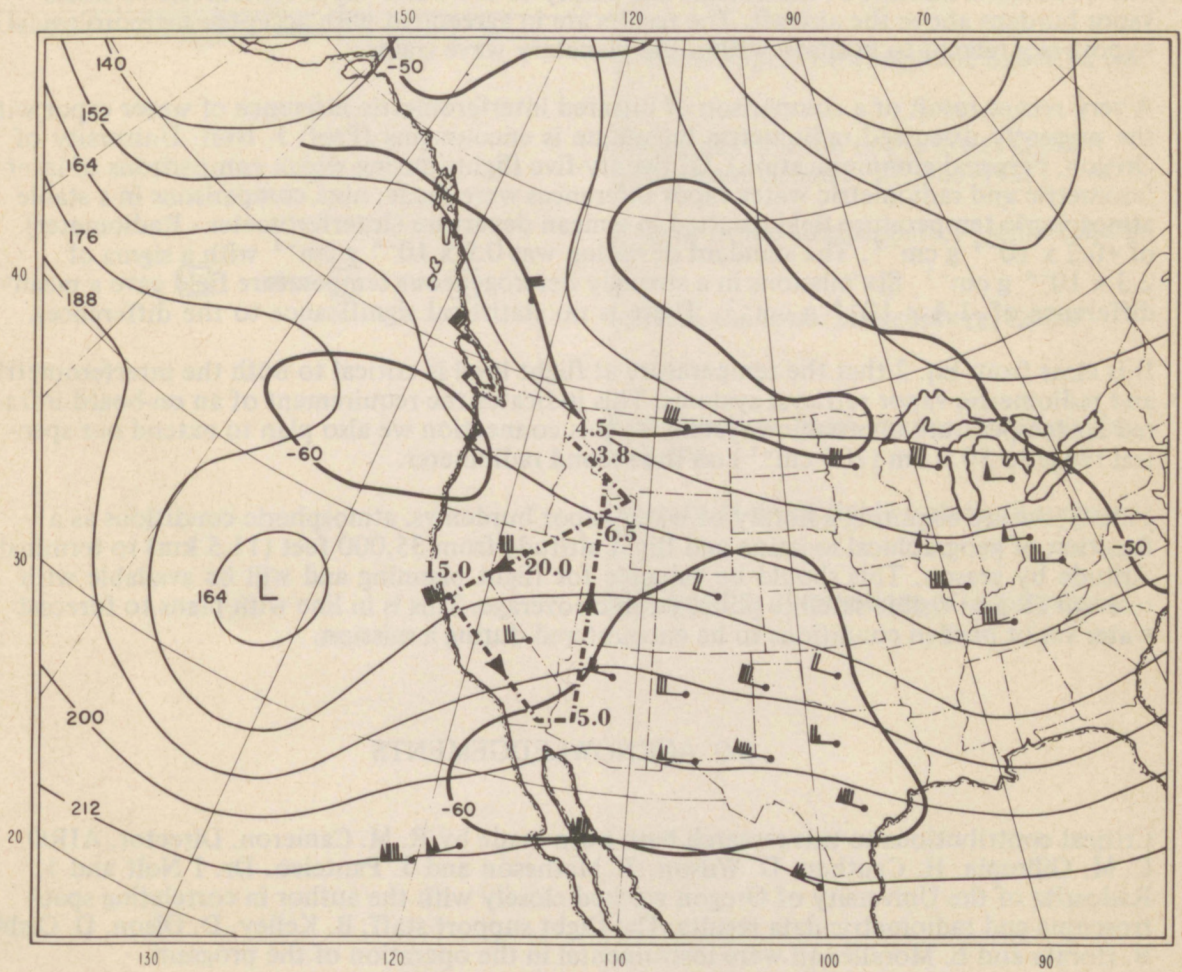


Figure 4. Water vapor burden (microns $\equiv 10^{-4} \text{ g cm}^{-2}$) 5 March 1975.

Along the track southwestward to San Francisco the influence of the deep trough and stationary low off the coast, with flow from the southwest around the low, indicated upwelling from the marine layer. The results from this flight follow classic meteorological concepts.

5.0 CONCLUSIONS

The two flights discussed demonstrate the ability of the water vapor radiometer to assess vapor burdens above the aircraft. The results are in agreement with accepted meteorological hypotheses related to position within the planetary wave trains.

A very recent result of a comparison of infrared interferometric inference of water vapor with the presently discussed radiometric technique is encouraging (Prof. J. Nolt, University of Oregon, personal communication). Of twenty-five flights during which comparisons of interferometric and radiometric water vapor inferences were made, nine comparisons in a stable atmospheric temperature field resulted in a mean departure (Interferometer - Radiometer) of $+0.2 \times 10^{-4} \text{ g cm}^{-2}$. The standard deviation was $0.9 \times 10^{-4} \text{ g cm}^{-2}$ with a sigma of $2.3 \times 10^{-4} \text{ g cm}^{-2}$. Six missions in a strongly heterogeneous temperature field gave a mean difference of $-1.4 \times 10^{-4} \text{ g cm}^{-2}$. There is no statistical significance to the differences.

It is clear from Eq. 2 that the temperature at flight level is critical to both the interferometric and radiometric vapor retrieval systems. This indicates the requirement of an on-board infrared air temperature observation system. In this connection we also plan to extend our spectral range to $50.0 \mu\text{m}$ (200 cm^{-1}) on the second radiometer.

Finally, we are acquiring a library of water vapor burden vs. atmospheric conditions as a function of geographical location and flight altitude from 35,000 feet (11.5 km) to terminal altitude by season. This should be valuable for flight planning and will be available with relevant IR and visible satellite photographic coverage. This is in line with plans to forecast water vapor burden conditions to be encountered during a mission.

6.0 ACKNOWLEDGEMENTS

Critical contributions to this research have been made by R. M. Cameron, Director, AIRO, C. M. Gillespie, H. Cauthen, D. Wilson, T. Matheson and J. Panteleo. Dr. I Nolt and J. Radostitz of the University of Oregon worked closely with the author in correlating spectroscopic and radiometric data results. The flight support staff, B. Kelley, D. Olson, D. Oishi, B. Horata and E. Morales all were instrumental in the operation of the program.

7.0 REFERENCES

- Brewer, A. W. and K. P. B. Tomson (1972): A radiometer-sonde for observing stratospheric emission due to water vapor in its rotational band, *Quart. J. Roy. Met. Soc.*, **98**, 187-192.
- Harries, J. E., D. G. Moss and N. R. Swann (1974): H₂O, O₃, N₂O and HNO₃ in the Arctic stratosphere, *Nature*, **250**, 475-476.
- Kuhn, P. M., M. S. Lojko and E. V. Petersen (1971): Water vapor: Stratospheric injection by thunderstorms, *Science*, **174**, 1319-1321.
- McKinnon, D. and H. W. Morewood (1970): Water vapor distribution in the lower stratosphere over North and South America, *J. Atmospheric Science*, **27**, 483-493.
- Mastenbrook, H. J. (1971): The variability of water vapor in the stratosphere, *J. Atmospheric Sci.*, **28**, 1495-1501.
- Mastenbrook, H. J. (1974): Water vapor measurements in the lower stratosphere, *Can. J. Chem*, **52**, 1527-1531.
- Ralston, A. and H. Wilf (1967): Multipoint iteration function, *Mathematical Methods for Digital Computers*, **2**, John Wiley and Sons, Inc.,
- Smith, W. L. (1966): Note on the relationship between total precipitable water and surface dew point, *J. Appl. Meteor.*, **5**, 726-727.
- Wark, D. Q., J. H. Liensch and M. P. Weinreb (1974): Satellite observations of atmospheric water vapor, *Appl. Optics*, **13**, 507-511.

PUBLICATION DATA AND FLOW

SELECTION			VERIFICATION-SEARCHING		PROCESSING	
ASL <input checked="" type="checkbox"/>	MESL <input type="checkbox"/>	MESL/F <input type="checkbox"/>	CARD CATALOG		N.A. TIL BOUND	
COPY NUMBER 1	COPY NUMBER	COPY NUMBER	TPB		REFERENCE	
CHIEF, ACQ. SECT. (Initials)		DATE 5-9	MESL		ADD TO S.L.	
INITIAL PROCESSING			CORPORATE		COMPUTER	
			PERSONAL		L.C. - XEROX COPY	
			TITLE		SEARCH	
			ASL		OTHER	
			DATE SEARCHED			
ACCESSION NUMBER	CATALOGUER (Initials)		DATE	LC CARD NUMBER		

CALL NUMBER: ASL MESL F

5. NOTES:

1. AUTHOR: ASL MESL F

6. ADDED ENTRIES:

2. TITLE:

CROSS REFERENCES: ASL MESL F

EDITION
3. IMPRINT:

COLLATION
4. SERIES:

REVIEWER'S INITIALS
CARDS TYPED
PROCESSING (Pocket, label, etc.)
PROOFING (Initials)
CHIEF, CATALOG SECT. (Initials)
ACCESSIONS LIST NO.